

Ferrous and cobaltous chloride complexes bearing 2-(1-(arylimino)methyl)-8-(1*H*-benzimidazol-2-yl)quinolines: Synthesis, characterization and catalytic behavior in ethylene polymerization

Tianpengfei Xiao^a, Shu Zhang^a, Baixiang Li^b, Xiang Hao^a, Carl Redshaw^{c,**},
Yue-Sheng Li^b, Wen-Hua Sun^{a,b,*}

^a Key Laboratory of Engineering Plastics and Beijing National Laboratory for Molecular Sciences, Institute of Chemistry, Chinese Academy of Science, Beijing 100190, China

^b State Key Laboratory of Polymer Physics and Chemistry, Changchun Institute of Applied Chemistry, Chinese Academy of Science, Changchun 130022, China

^c School of Chemistry, University of East Anglia, Norwich NR4 7TJ, UK

ARTICLE INFO

Article history:

Received 28 August 2011
Received in revised form
11 October 2011
Accepted 20 October 2011
Available online 25 October 2011

Keywords:

2-Imino-8-benzimidazolylquinolines
Late-transition metal complex
Ethylene polymerization

ABSTRACT

The series of ligands 2-(1-(arylimino)methyl)-8-(1*H*-benzimidazol-2-yl)quinolines was synthesized and used to prepare new iron(II) and cobalt(II) dichloride complexes. X-ray diffraction studies revealed that the coordination geometry around the metal center can best be described as distorted square-based pyramidal. Upon activation with methylaluminoxane (MAO), both families (Fe and Co) of complexes showed good activities in ethylene polymerization, affording highly linear polyethylenes. Enhanced activities were observed on increasing the reaction temperature to 100 °C. The optimization of the reaction parameters and the influence of the substituents on the imino-bound aryl group of the chelate ligands were investigated.

© 2011 Elsevier Ltd. All rights reserved.

1. Introduction

The discovery of bis(imino)pyridine complexes of iron(II) and cobalt(II) as highly active pro-catalysts in ethylene polymerization [1,2] provided a landmark from the view of both polyolefins and catalysis [3–8]. In particular, notwithstanding their high activity, ferrous pro-catalysts have been explored for ethylene oligomerization due to their high selectivity for linear α -olefins [3]. Numerous modifications of the bis(imino)pyridine framework have been made in order to improve the catalytic performance of the complexes [3–8]. Such modifications illustrate the influence of the steric and electronic properties of the substituents on the catalytic behaviour of the metal complexes [9–14], which can lead to the formation of either high molecular weight polyethylene and/or oligomeric products [3–14]. Alternative models of the pro-catalysts have relied on designing new tridentate ligands, and indeed, we have reported highly active metal pro-catalysts bearing ligands such as

2-imino-1,10-phenanthrolines [15–19], 2-(benzimidazol-2-yl)-1,10-phenanthrolines [20], 2-benzimidazolyl-6-iminopyridines [21–24], 2-benzoxazolyl-6-iminopyridines [25,26], 2-quinoxaliny-6-iminopyridines [27], 2-methyl-2,4-bis-(6-iminopyridin-2-yl)-1*H*-1,5-benzodiazepines [28,29], iminoquinolines [30], 2,8-bis(imino)quinoline [31], and 8-(2-benzimidazolyl)-quinolines [32,33].

Despite these advances, the critical problem of the poor thermal stability of such iron and cobalt systems remained, and the resultant dramatic decreases in both catalyst activities and polymer molecular weight at increased reaction temperatures were clearly a hurdle to potential industrial application [3–14]. Given this, catalytic development is targeted the thermally stable systems [34–37], and variation of the substituents at the *ortho*-position of the iminoaryl groups was mostly probed [38–42]. Moreover, new ligand frameworks have been created [43–49], and indeed the metal pro-catalysts bearing the 2,8-bis(imino)quinoline ligands exhibited optimized performance at high temperature (100 °C) for ethylene polymerization [31]. Encouraged by the results obtained by pro-catalysts bearing the 2,8-bis(imino)quinoline ligand system [31], as well as for those bearing 2-benzimidazolyl-6-iminopyridines [21–24], a series of 2-(1-(arylimino)methyl)-8-(1*H*-benzimidazol-2-yl)quinoline ligands were synthesized and the iron and cobalt complexes thereof prepared. When activated with methylaluminoxane (MAO), these complexes exhibit good

* Corresponding author. Key Laboratory of Engineering Plastics and Beijing National Laboratory for Molecular Sciences, Institute of Chemistry, Chinese Academy of Science, Beijing 100190, China. Tel.: +86 1062557955; fax: +86 1062618239.

** Corresponding author. Fax: +44 (0) 1603 592003.

E-mail addresses: carl.redshaw@uea.ac.uk (C. Redshaw), whsun@iccas.ac.cn (W.-H. Sun).

activities for ethylene polymerization, especially at higher reaction temperatures. Herein, we report the synthesis and characterization of the 2-(1-(arylimino)methyl)-8-(1*H*-benzimidazol-2-yl)quinoline ligands, together with their ferrous and cobaltous complexes, and investigate their catalytic performance in ethylene polymerization.

2. Experimental

2.1. General considerations

All manipulations of air- and moisture-sensitive compounds were performed under a nitrogen atmosphere using standard Schlenk techniques. Toluene was refluxed over sodium-benzophenone and distilled under argon prior to use. Methylaluminoxane (MAO, a 1.46 M solution in toluene) was purchased from Akzo Nobel Corp. ¹H and ¹³C NMR spectra were recorded on a Bruker DMX 400 MHz instrument at ambient temperature using TMS as an internal standard. IR spectra were recorded on a Perkin–Elmer System 2000 FT-IR spectrometer. Elemental analysis was carried out by using a Flash EA 1112 microanalyzer. DSC trace and melting points of polyethylene were obtained from the second scanning run on Perkin–Elmer DSC-7 at a heating rate of 10 °C/min. Molecular weights and molecular weight distribution of polyethylenes were determined by a PL-GPC220 at 135 °C with 1,2,4-trichlorobenzene as the solvent.

2.2. Preparation of the ligands

2.2.1. 2-(1-(2,6-Dimethylphenylimino)methyl)-8-(1*H*-benzimidazol-2-yl)quinoline (**L1**)

Both 2,6-dimethylaniline (0.456 g, 3.77 mmol) and *p*-toluenesulfonic acid (0.010 g) were added to a solution of 2-formyl-8-(1*H*-benzimidazol-2-yl)quinoline [50] (0.686 g, 2.51 mmol) in toluene, using 4 Å molecular sieves as the water absorption agent. The reaction mixture was refluxed for 12 h under an N₂ atmosphere. After the reaction was stopped, the solvent was removed and the residue was eluted on an alumina column (petrol ether/ethyl acetate (v/v) 10:1). **L1** (0.5043 g, 1.36 mmol) was obtained in 54.3% yield as a yellow solid. m.p. 114–116 °C; FT-IR (KBr Disc): $\nu = 3286, 3051, 1644, 1593, 1567, 1401, 1315, 1194, 856, 742, 655 \text{ cm}^{-1}$; ¹H NMR (400 MHz, CDCl₃, 25 °C, TMS): $\delta = 13.32$ (br, 1H, NH), 9.22 (d, ³J(H,H) = 7.4 Hz, 1H, quin), 8.69 (s, 1H, ArN=CH), 8.50 (d, ³J(H,H) = 8.6 Hz, 1H, quin), 8.45 (d, ³J(H,H) = 8.6 Hz, 1H, quin), 8.01 (d, ³J(H,H) = 8.1 Hz, 1H, quin), 7.91–7.85 (m, 1H, aryl), 7.81 (t, ³J(H,H) = 7.8 Hz, 1H, quin), 7.64–7.56 (m, 1H, aryl), 7.35–7.25 (m, 2H, aryl), 7.18 (d, ³J(H,H) = 7.5 Hz, 2H, aryl), 7.07 (t, ³J(H,H) = 7.3 Hz, 1H, aryl), 2.26 ppm (s, 6H, CH₃); ¹³C{¹H} NMR (100 MHz, CDCl₃, 25 °C, TMS): $\delta = 162.9, 153.8, 151.0, 150.3, 144.9, 143.2, 138.4, 134.2, 131.0, 129.8, 129.7, 128.3, 128.1, 126.8, 126.4, 124.6, 123.2, 122.5, 119.5, 118.6, 111.5, 18.4$ ppm; Elemental analysis: calcd. (%) for C₂₅H₂₀N₄ (376.5): C 79.76, H 5.35, N 14.88; Found: C 79.75, H 5.44, N 14.76.

2.2.2. 2-(1-(2,6-Diethylphenylimino)methyl)-8-(1*H*-benzimidazol-2-yl)quinoline (**L2**)

As for the synthesis of **L1**, **L2** was obtained in the similar manner in 49.3% yield as the yellow solid. m.p. 117–119 °C; FT-IR (KBr Disc): $\nu = 3291, 3056, 1632, 1589, 1569, 1432, 1315, 1276, 1120, 845, 771, 740, 658 \text{ cm}^{-1}$; ¹H NMR (400 MHz, CDCl₃, 25 °C, TMS): $\delta = 13.34$ (br, 1H, NH), 9.22 (d, ³J(H,H) = 7.3 Hz, 1H, quin), 8.69 (s, 1H, ArN=CH), 8.49 (d, ³J(H,H) = 8.5 Hz, 1H, quin), 8.45 (d, ³J(H,H) = 8.5 Hz, 1H, quin), 8.01 (d, ³J(H,H) = 7.8 Hz, 1H, quin), 7.90–7.86 (m, 1H, aryl), 7.81 (t, ³J(H,H) = 7.8 Hz, 1H, quin), 7.57–7.53 (m, 1H, aryl), 7.33–7.27 (m, 2H, aryl), 7.20 (d, ³J(H,H) = 7.5 Hz, 2H, aryl), 7.15 (t, ³J(H,H) = 7.4 Hz, 1H, aryl), 2.61 (q, ³J(H,H) = 7.5 Hz, 4H, CH₂CH₃), 1.22 ppm (t, ³J(H,H) = 7.5 Hz, 6H, CH₂CH₃); ¹³C{¹H} NMR (100 MHz,

CDCl₃, 25 °C, TMS): $\delta = 162.8, 154.3, 151.6, 150.1, 145.5, 143.7, 139.1, 134.6, 133.3, 131.6, 130.3, 130.2, 128.8, 127.0, 125.4, 123.7, 123.0, 120.1, 119.2, 111.9, 25.3, 15.1$ ppm; Elemental analysis: calcd. (%) for C₂₇H₂₄N₄ (404.5): C 80.17, H 5.98, N 13.85; Found: C 80.21, H 6.18, N 13.56.

2.2.3. 2-(1-(2,6-Diisopropylphenylimino)methyl)-8-(1*H*-benzimidazol-2-yl)quinoline (**L3**)

As for the synthesis of **L1**, **L3** was obtained in the similar manner in 70.0% yield as the yellow solid. m.p. 121–123 °C; FT-IR (KBr Disc): $\nu = 3280, 3065, 1637, 1589, 1570, 1431, 1316, 1276, 1178, 848, 767, 739 \text{ cm}^{-1}$; ¹H NMR (400 MHz, CDCl₃, 25 °C, TMS): $\delta = 13.36$ (br, 1H, NH), 9.21 (d, ³J(H,H) = 7.3 Hz, 1H, quin), 8.66 (s, 1H, ArN=CH), 8.47 (d, ³J(H,H) = 8.5 Hz, 1H, quin), 8.44 (d, ³J(H,H) = 8.5 Hz, 1H, quin), 7.99 (d, ³J(H,H) = 7.9 Hz, 1H, quin), 7.90–7.84 (m, 1H, aryl), 7.80 (t, ³J(H,H) = 7.7 Hz, 1H, quin), 7.55–7.49 (m, 1H, aryl), 7.32–7.27 (m, 2H, aryl), 7.24 (d, ³J(H,H) = 7.5 Hz, 2H, aryl), 7.22 (t, ³J(H,H) = 7.4 Hz, 1H, aryl), 3.08 (sept, ³J(H,H) = 7.5 Hz, 2H, CH(CH₃)₂), 1.26 ppm (d, ³J(H,H) = 6.8 Hz, 12H, CH(CH₃)₂); ¹³C{¹H} NMR (100 MHz, CDCl₃, 25 °C, TMS): $\delta = 162.3, 153.7, 151.1, 148.5, 145.0, 143.2, 138.6, 137.3, 134.1, 131.1, 129.8, 129.7, 128.3, 126.5, 125.1, 123.4, 123.2, 122.5, 119.6, 118.8, 111.3, 28.2, 23.5$ ppm; Elemental analysis: calcd. (%) for C₂₉H₂₈N₄ (432.6): C 80.52, H 6.52, N 12.95; Found: C 80.61, H 6.58, N 12.56.

2.2.4. 2-(1-(2,4,6-Trimethylphenylimino)methyl)-8-(1*H*-benzimidazol-2-yl)quinoline (**L4**)

As for the synthesis of **L1**, **L4** was obtained in the similar manner in 53.9% yield as the yellow solid. m.p. 118–120 °C; FT-IR (KBr Disc): $\nu = 3236, 3065, 1640, 1591, 1569, 1433, 1319, 1277, 1205, 1141, 845, 766, 740 \text{ cm}^{-1}$; ¹H NMR (400 MHz, CDCl₃, 25 °C, TMS): $\delta = 13.34$ (br, 1H, NH), 9.21 (d, ³J(H,H) = 7.4 Hz, 1H, quin), 8.68 (s, 1H, ArN=CH), 8.49 (d, ³J(H,H) = 8.5 Hz, 1H, quin), 8.44 (d, ³J(H,H) = 8.3 Hz, 1H, quin), 8.00 (d, ³J(H,H) = 8.0 Hz, 1H, quin), 7.92–7.85 (m, 1H, aryl), 7.81 (t, ³J(H,H) = 7.7 Hz, 1H, quin), 7.60–7.53 (m, 1H, aryl), 7.35–7.27 (m, 2H, aryl), 7.00 (s, 2H, aryl), 2.35 (s, 3H, CH₃), 2.23 ppm (s, 6H, CH₃); ¹³C{¹H} NMR (100 MHz, CDCl₃, 25 °C, TMS): $\delta = 162.7, 153.8, 151.0, 147.9, 144.9, 143.2, 138.3, 134.1, 131.0, 129.7, 129.6, 129.0, 128.1, 126.7, 126.4, 123.1, 122.4, 119.5, 118.6, 111.4, 108.8, 20.8, 18.3$ ppm; Elemental analysis: calcd. (%) for C₂₆H₂₂N₄ (390.5): C 79.97, H 5.68, N 14.35; Found: C 80.11, H 5.58, N 14.56.

2.2.5. 2-(1-(2,6-Difluorophenylimino)methyl)-8-(1*H*-benzimidazol-2-yl)quinoline (**L5**)

2-formyl-8-(1*H*-benzimidazol-2-yl)quinoline (0.7253 g, 2.66 mmol), 2,6-difluoroaniline (0.5147 g, 3.99 mmol), and *p*-toluenesulfonic acid (0.030 g) were combined with tetraethyl silicate (5 mL) in a flask. The flask was equipped with a condenser along with a water knockout trap, and the mixture was refluxed under nitrogen for 28 h. Tetraethyl silicate was removed at reduced pressure, and the resulting solid was eluted with petroleum ether/ethyl acetate (v/v) 10:1 on an alumina column. The second eluting part was collected and concentrated to give a yellow solid in 24.5% yield. m.p. 125–127 °C; FT-IR (KBr Disc): $\nu = 3258, 3060, 1635, 1575, 1433, 1327, 1278, 1147, 850, 809, 769, 741 \text{ cm}^{-1}$; ¹H NMR (400 MHz, CDCl₃, 25 °C, TMS): $\delta = 13.26$ (br, 1H, NH), 9.23 (d, ³J(H,H) = 7.3 Hz, 1H, quin), 8.84 (s, 1H, ArN=CH), 8.51–8.41 (m, 2H, quin), 8.00 (d, ³J(H,H) = 8.0 Hz, 1H, quin), 7.94–7.84 (m, 1H, aryl), 7.82 (t, ³J(H,H) = 7.7 Hz, 1H, quin), 7.67–7.56 (m, 1H, aryl), 7.46 (d, ³J(H,H) = 8.0 Hz, 2H, aryl), 7.36–7.27 (m, 2H, aryl), 7.12 ppm (t, ³J(H,H) = 8.0 Hz, 1H, aryl); ¹³C{¹H} NMR (100 MHz, CDCl₃, 25 °C, TMS): $\delta = 165.6, 156.9, 154.4, 153.7, 151.1, 145.1, 143.3, 138.5, 134.4, 131.2, 129.8, 128.5, 126.8, 123.2, 122.6, 119.6, 119.4, 112.4, 112.2, 111.6$ ppm; Elemental analysis: calcd. (%) for C₂₃H₁₄F₂N₄ (384.4): C 71.87, H 3.67, N 14.58; Found: C 71.49, H 3.75, N 14.23.

2.2.6. 2-(1-(2,6-Dichlorophenylimino)methyl)-8-(1H-benzimidazol-2-yl)quinoline (**L6**)

As for the synthesis of **L5**, **L6** was obtained in the similar manner in 23.7% yield as the yellow solid. m.p. 130–132 °C; FT-IR (KBr Disc): $\nu = 3319, 3059, 1637, 1563, 1425, 1327, 1260, 1143, 1019, 843, 764, 738 \text{ cm}^{-1}$; $^1\text{H NMR}$ (400 MHz, CDCl_3 , 25 °C, TMS): $\delta = 13.36$ (br, 1H, NH), 9.21 (d, $^3J(\text{H,H}) = 7.2 \text{ Hz}$, 1H, quin), 9.12 (s, 1H, ArN=CH), 8.42 (s, 2H, quin), 7.98 (d, $^3J(\text{H,H}) = 7.9 \text{ Hz}$, 1H, quin), 7.93–7.84 (m, 1H, aryl), 7.80 (t, $^3J(\text{H,H}) = 7.5 \text{ Hz}$, 1H, quin), 7.68–7.58 (m, 1H, aryl), 7.39–7.27 (m, 2H, aryl), 7.23–7.16 (m, 1H, aryl), 7.14–7.02 ppm (m, 2H, aryl); $^{13}\text{C}\{^1\text{H}\}$ NMR (100 MHz, CDCl_3 , 25 °C, TMS): $\delta = 166.4, 153.1, 151.0, 146.5, 145.1, 143.3, 138.7, 134.3, 131.4, 130.0, 129.8, 128.7, 126.8, 126.0, 125.8, 123.3, 122.6, 119.7, 119.3, 111.7 \text{ ppm}$; Elemental analysis: calcd. (%) for $\text{C}_{23}\text{H}_{14}\text{Cl}_2\text{N}_4$ (417.3): C 66.20, H 3.38, N 13.43; Found: C 66.15, H 3.75, N 13.23.

2.3. Synthesis of the iron complexes **Fe1** – **Fe6**

The stoichiometric reaction of ligand and $\text{FeCl}_2 \cdot 4\text{H}_2\text{O}$ was carried out in a Schlenk tube, which was purged three times with N_2 and then charged with freshly distilled THF. The reaction mixture was stirred at room temperature for 10 h. The resulting precipitate was filtered, washed with diethyl ether three times, and dried in a vacuum at 60 °C. All the iron(II) complexes (**Fe1** – **Fe6**) were prepared in high yields in this manner. Data for iron complexes are as follows:

Complex **Fe1** was obtained as a green powder in 72.4% yield. FT-IR (KBr Disc): $\nu = 3116, 1621, 1589, 1519, 1434, 1406, 1326, 1176, 986, 865, 743 \text{ cm}^{-1}$; Elemental analysis: calcd. (%) for $\text{C}_{25}\text{H}_{20}\text{Cl}_2\text{FeN}_4$ (503.2): C 59.67, H 4.01, N 11.13; Found: C 59.49, H 4.12, N 10.77.

Complex **Fe2** was obtained as a green powder in 84.4% yield. FT-IR (KBr Disc): $\nu = 3103, 1625, 1592, 1517, 1432, 1324, 987, 848, 749 \text{ cm}^{-1}$; Elemental analysis: calcd. (%) for $\text{C}_{27}\text{H}_{24}\text{Cl}_2\text{FeN}_4$ (531.3): C 61.04, H 4.55, N 10.55; Found: C 61.24, H 4.75, N 10.36.

Complex **Fe3** was obtained as a green powder in 87.4% yield. FT-IR (KBr Disc): $\nu = 3168, 1629, 1592, 1518, 1434, 1323, 985, 861, 745 \text{ cm}^{-1}$; Elemental analysis: calcd. (%) for $\text{C}_{29}\text{H}_{28}\text{Cl}_2\text{FeN}_4$ (559.3): C 62.27, H 5.05, N 10.02; Found: C 62.25, H 5.01, N 9.79.

Complex **Fe4** was obtained as a green powder in 88.1% yield. FT-IR (KBr Disc): $\nu = 3168, 1619, 1592, 1437, 1325, 1214, 1143, 990, 848, 734 \text{ cm}^{-1}$; Elemental analysis: calcd. (%) for $\text{C}_{26}\text{H}_{22}\text{Cl}_2\text{FeN}_4$ (517.2): C 60.38, H 4.29, N 10.83; Found: C 60.33, H 4.33, N 10.96.

Complex **Fe5** was obtained as a green powder in 85.8% yield. FT-IR (KBr Disc): $\nu = 3143, 1613, 1590, 1528, 1146, 842, 685 \text{ cm}^{-1}$; Elemental analysis: calcd. (%) for $\text{C}_{23}\text{H}_{14}\text{Cl}_2\text{F}_2\text{FeN}_4$ (511.1): C 54.05, H 2.76, N 10.96; Found: C 54.33, H 2.85, N 10.73.

Complex **Fe6** was obtained as a green powder in 80.7% yield. FT-IR (KBr Disc): $\nu = 3059, 1613, 1531, 1569, 1514, 1454, 1404, 850, 773, 749 \text{ cm}^{-1}$; Elemental analysis: calcd. (%) for $\text{C}_{23}\text{H}_{14}\text{Cl}_4\text{FeN}_4$ (544.0): C 50.78, H 2.59, N 10.30; Found: C 50.68, H 2.83, N 10.31.

2.4. Synthesis of the cobalt complexes **Co1** – **Co6**

The solution of CoCl_2 in ethanol was added to a solution of ligand **L1** at room temperature, and the solution turned blue immediately. After the reaction mixture was stirred for 10 h, diethyl ether was added into the mixture. The resultant precipitate was filtered, washed with diethyl ether and dried in a vacuum to obtain the pure product. All the cobalt (II) complexes (**Co1** – **Co6**) were prepared in high yields in this manner. Data for cobalt complexes are as follows:

Complex **Co1** was obtained as a yellow powder in 88.2% yield. FT-IR (KBr Disc): $\nu = 3112, 1625, 1593, 1512, 1436, 1327, 1147, 992, 850, 749 \text{ cm}^{-1}$; Elemental analysis: calcd. (%) for $\text{C}_{25}\text{H}_{20}\text{Cl}_2\text{CoN}_4$ (506.3): C 59.31, H 3.98, N 11.07; Found: C 59.04, H 4.38, N 11.36.

Complex **Co2** was obtained as a yellow powder in 91.8% yield. FT-IR (KBr Disc): $\nu = 3107, 1620, 1589, 1507, 1434, 1327, 1222, 988, 870, 750 \text{ cm}^{-1}$. Elemental analysis: calcd. (%) for $\text{C}_{27}\text{H}_{24}\text{Cl}_2\text{CoN}_4$ (534.4): C 60.69, H 4.53, N 10.49; Found: C 60.96, H 4.67, N 10.14.

Complex **Co3** was obtained as a yellow powder in 90.3% yield. FT-IR (KBr Disc): $\nu = 3166, 1624, 1590, 1523, 1435, 1327, 1221, 990, 856, 762 \text{ cm}^{-1}$; Elemental analysis: calcd. (%) for $\text{C}_{29}\text{H}_{28}\text{Cl}_2\text{CoN}_4$ (562.4): C 61.93, H 5.02, N 9.96; Found: C 61.72, H 5.24, N 9.63.

Complex **Co4** was obtained as a yellow powder in 87.4% yield. FT-IR (KBr Disc): $\nu = 3121, 1627, 1594, 1526, 1439, 1330, 1221, 993, 850, 768 \text{ cm}^{-1}$; Elemental analysis: calcd. (%) for $\text{C}_{26}\text{H}_{22}\text{Cl}_2\text{CoN}_4$ (520.3): C 60.02, H 4.26, N 10.77; Found: C 59.98, H 4.28, N 10.66.

Complex **Co5** was obtained as a yellow powder in 86.1% yield. FT-IR (KBr Disc): $\nu = 3062, 1635, 1590, 1514, 1433, 1322, 1212, 987, 861, 762 \text{ cm}^{-1}$; Elemental analysis: calcd. (%) for $\text{C}_{23}\text{H}_{14}\text{Cl}_2\text{F}_2\text{CoN}_4$ (514.2): C 53.72, H 2.74, N 10.90; Found: C 53.76, H 2.95, N 10.67.

Complex **Co6** was obtained as a yellow powder in 79.4% yield. FT-IR (KBr Disc): $\nu = 3059, 1635, 1593, 1516, 1436, 1326, 1214, 988, 857, 763 \text{ cm}^{-1}$; Elemental analysis: calcd. (%) for $\text{C}_{23}\text{H}_{14}\text{Cl}_4\text{CoN}_4$ (547.1): C 50.49, H 2.58, N 10.24; Found: C 50.69, H 2.92, N 10.35.

2.5. Procedure for ethylene polymerization

Ethylene polymerization were performed in a stainless steel autoclave (0.25 L capacity) equipped with a mechanical stirrer and a temperature controller. A 100 mL amount of toluene containing the catalyst precursor was transferred to the fully dried reactor under nitrogen atmosphere. The required amount of co-catalyst was then injected into the reactor via a syringe. At the required reaction temperature, the reactor was immediately pressurized to high ethylene pressure, and the ethylene pressure was kept constant with feeding of ethylene. After the reaction mixture was stirred for the desired period, the pressure was released and the mixture was cooled to room temperature. Following this, the residual reaction solution was quenched with 30% hydrochloride acid ethanol, and then the precipitated polymer was collected by filtration, and was adequately washed with ethanol and water, and was dried in a vacuum until of constant weight.

2.6. X-ray crystallographic Study

Data were collected with an MM007-HF CCD (Saturn 724+) diffractometer with graphite monochromated Mo-K α radiation ($\lambda = 0.71073 \text{ \AA}$) at 173(2) K. Cell parameters were obtained by global refinement of the positions of all collected reflections. Intensities were corrected for Lorentz and polarization effects and empirical absorption. The structures were solved by direct methods and refined by full-matrix least-squares on F^2 . All hydrogen atoms were placed in calculated positions. Structure solution and refinement were performed by using the SHELXL-97 package [51]. Crystal data and processing parameters for of **Fe1**, **Fe4**, **Co2**, **Co3** and **Co4** are summarized in Table 1.

3. Results and discussion

3.1. Synthesis and characterization of ligands and complexes

The 2-(1-(arylimino)methyl)-8-(1H-benzimidazol-2-yl)quinoline ligands (**L1**–**L6**) were synthesized in satisfactory yields through the condensation reaction of 2-formyl-8-(1H-benzimidazol-2-yl)quinoline with the corresponding anilines, in the presence of a catalytic amount of *p*-toluenesulfonic acid. However, adaptations were necessary using different solvents and water absorbing reagents in order to improve the yields. All ligands (**L1**–**L6**) were consistent with their elemental analyses and were characterized by

Table 1
Crystal data and structure refinement for **Fe1**, **Fe4**, **Co2**, **Co3** and **Co4**.

	Fe1	Fe4	Co2	Co3	Co4
CCDC No.	829448	829449	829450	829451	829452
Empirical formula	C ₂₅ H ₂₀ Cl ₂ FeN ₄	C ₂₆ H ₂₂ Cl ₂ FeN ₄	C ₂₇ H ₂₄ Cl ₂ CoN ₄	C ₂₉ H ₂₈ Cl ₂ CoN ₄	C ₂₆ H ₂₂ Cl ₂ CoN ₄
Fw	503.20	517.23	534.33	562.38	520.31
Crystal color	green	green	black	brown	brown
Crystal system	Monoclinic	Monoclinic	Monoclinic	Monoclinic	Monoclinic
space group	P2(1)/n	P2(1)/c	P2(1)/c	P2(1)/n	P2(1)/c
a (Å)	12.955(3)	18.312(4)	7.3558(15)	13.000(3)	18.486(4)
b (Å)	10.611(2)	7.4549(15)	19.744(4)	14.352(3)	7.3998(15)
c (Å)	16.057(3)	16.962(3)	16.566(3)	14.380(3)	16.828(3)
β (°)	98.51(3)	90.53(3)	94.37(3)	93.00(3)	90.90(3)
Volume (Å ³)	2182.9(8)	2315.5(8)	2399.0(8)	2679.3(9)	2301.7(8)
Z	4	4	4	4	4
Dcalc(Mg m ⁻³)	1.531	1.484	1.479	1.394	1.501
μ (mm ⁻¹)	0.957	0.905	0.962	0.865	1.000
F(000)	1032	1064	1100	1164	1068
Crystal size (mm)	0.22 × 0.21 × 0.06	0.12 × 0.07 × 0.01	0.13 × 0.12 × 0.12	0.28 × 0.21 × 0.21	0.11 × 0.11 × 0.02
θ range (°)	1.89–27.48	2.22–27.47	1.61–27.46	2.01–27.45	2.20–27.50
Limiting indices	−16 ≤ h ≤ 16, −13 ≤ k ≤ 13, −13 ≤ l ≤ 20	−23 ≤ h ≤ 23, −8 ≤ k ≤ 9, −19 ≤ l ≤ 22	−9 ≤ h ≤ 7, −25 ≤ k ≤ 25, −15 ≤ l ≤ 21	−16 ≤ h ≤ 16, −16 ≤ k ≤ 18, −18 ≤ l ≤ 18	−24 ≤ h ≤ 16, −9 ≤ k ≤ 9, −21 ≤ l ≤ 18
Completeness to θ (%)	99.7 (θ = 27.48)	99.8 (θ = 27.47)	97.3 (θ = 27.46)	99.2 (θ = 27.45)	97.7 (θ = 27.05)
Absorption correction	Empirical	Empirical	Empirical	Empirical	Empirical
Data/restraints	4997/0/289	5298/0/298	5348/0/307	6083/0/325	5168/0/298
/parameters					
Goodness-of-fit on F ²	1.088	1.179	1.097	1.112	1.165
Final R indices	R1 = 0.0469, [I > 2σ(I)] wR2 = 0.1139	R1 = 0.0989, wR2 = 0.1675	R1 = 0.0487, wR2 = 0.0981	R1 = 0.0416, wR2 = 0.0978	R1 = 0.0817, wR2 = 0.1753
R indices (all data)	R1 = 0.0510, wR2 = 0.1172	R1 = 0.1365, wR2 = 0.1839	R1 = 0.0550, wR2 = 0.1018	R1 = 0.0446, wR2 = 0.0999	R1 = 0.0953, wR2 = 0.1843
Largest diff peak and hole (e Å ⁻³)	0.454 and −0.597	0.443 and −0.641	0.317 and −0.513	0.401 and −0.621	0.521 and −0.790

¹H and ¹³C NMR spectroscopy as well as by FT-IR, in which the C=N stretching frequencies appeared in the range of 1632–1644 cm⁻¹.

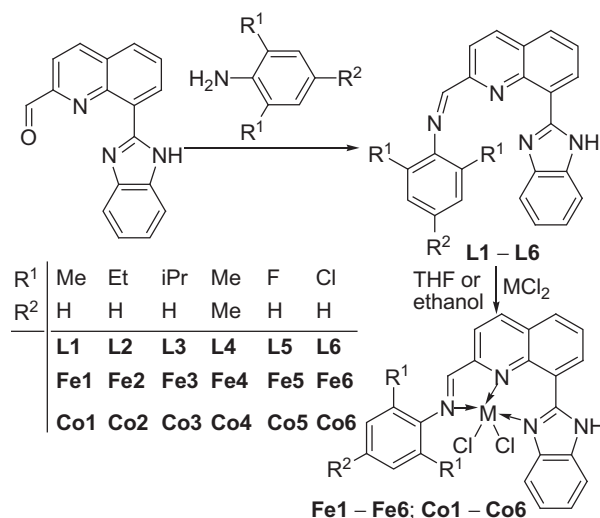
The metal complexes were synthesized by mixing the corresponding ligands with one equivalent of MCl₂ in suitable solvents (Scheme 1), and the resultant products were precipitated from the solution and collected via filtration. All iron complexes **Fe1–Fe6** were formed as green solids, and were stable in the solid state. However, solutions slowly changed from green to yellow, due to the oxidation of Fe^{II} to Fe^{III}. The cobalt analogs **Co1–Co6** were yellow powders and stable in both solution and the solid state.

All metal complexes were obtained in good yields, and were of sufficient purity (elemental analyses) for further use. Compared with the corresponding ligands, the stretching vibration bands of C=N of these metal complexes in the IR spectra shifted to lower frequencies in the range 1613–1629 cm⁻¹, and with the greatly reduced intensities, indicating the effective coordination between the imino-nitrogen and the metal. Moreover, the molecular structures of complexes **Fe1**, **Fe4** and **Co2–4** were confirmed by the single crystal X-ray diffraction.

3.2. X-ray crystallographic studies

Single crystals of **Fe1**, **Fe4** and **Co2–4** suitable for the X-ray diffraction analysis were obtained by slow diffusion of diethyl ether into the methanol solutions. In the case of iron, it was necessary for the complexes to be crystallized under a nitrogen atmosphere. The X-ray crystallographic studies revealed that all metal complexes can be described as adopting a pseudo square-based pyramidal geometry at the metal, in which the square base is comprised of the three coordinating nitrogen atoms of the chelate ligand and one chloride, whilst the other chloride atom is at the apical position. For comparison, selected bond lengths and angles are tabulated in Table 2.

As shown in Fig. 1, the iron atom in **Fe1** is coordinated with five atoms comprising three nitrogen atoms and two chlorides within a pseudo square-pyramid. The square-basal atoms of N1, N2, N3 and Cl2 are almost co-planar with a deviation of less than 0.2 Å, whilst the iron lies 0.438 Å out of the basal plane (Cl2–N1–N2–N3). The plane of three nitrogen atoms (N1, N2, and N3) is almost co-planar with the quinolinyl plane with the dihedral angle of ca. 7.86°. Considering the Fe–Cl bond lengths, the longer bond is to the apical chloride (2.3705(8) Å), compared to that to the basal counterpart (2.2973(10) Å). The coordination of the benzimidazole group with iron centre is via an sp² nitrogen (N3) instead



Scheme 1. Synthetic procedure for 2-(1-(arylimino)methyl)-8-(benzimidazolyl)-2-olines and their metal complexes.

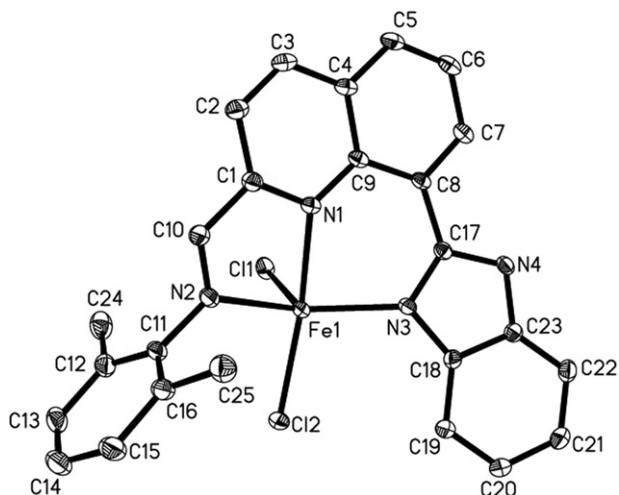
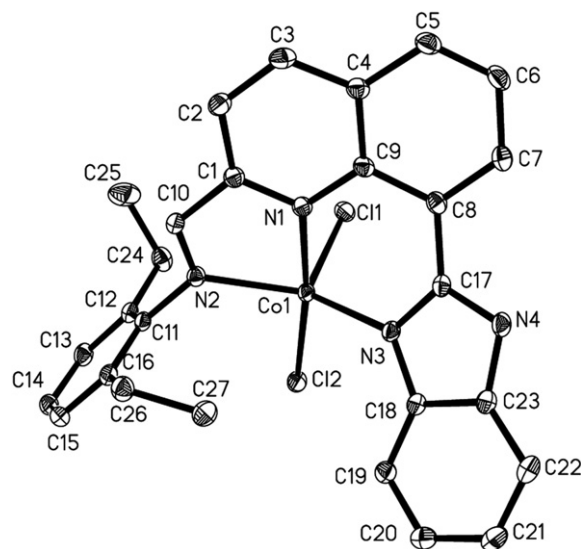
Table 2
Selected bond lengths (Å) and angles (°) for **Fe1**, **Fe4**, **Co2**, **Co3**, and **Co4**.

	Fe1	Fe4	Co2	Co3	Co4
Bond lengths (Å)					
M–N1	2.202(2)	2.201(4)	2.165(2)	2.1873(17)	2.175(4)
M–N2	2.179(2)	2.153(5)	2.112(2)	2.1279(16)	2.122(4)
M–N3	2.119(2)	2.079(4)	2.066(2)	2.0726(17)	2.055(4)
M–Cl1	2.3705(8)	2.3461(17)	2.3323(8)	2.3540(7)	2.3358(14)
M–Cl2	2.2973(10)	2.3356(17)	2.3021(10)	2.2979(9)	2.3149(14)
N1–C1	1.338(3)	1.335(6)	1.333(3)	1.336(2)	1.322(5)
N1–C9	1.366(3)	1.365(6)	1.355(3)	1.357(2)	1.360(6)
N2–C10	1.274(3)	1.284(7)	1.279(3)	1.283(2)	1.281(6)
N2–C11	1.447(3)	1.444(6)	1.450(3)	1.449(2)	1.444(6)
N3–C17	1.342(3)	1.334(6)	1.333(3)	1.343(2)	1.342(6)
N3–C18	1.410(3)	1.415(7)	1.405(3)	1.407(2)	1.403(6)
Bond angles (°)					
N1–M–N2	75.38(8)	74.70(17)	75.11(8)	75.52(6)	75.59(14)
N1–M–N3	83.18(8)	81.47(17)	82.05(8)	82.25(6)	82.38(15)
N2–M–N3	142.00(8)	133.22(17)	132.17(8)	131.86(6)	133.08(15)
N1–M–Cl1	91.32(6)	89.44(13)	88.77(6)	83.82(4)	86.66(11)
N1–M–Cl2	163.05(6)	169.49(13)	171.62(6)	175.25(4)	173.12(11)
N2–M–Cl1	102.21(6)	105.25(14)	109.50(6)	104.45(5)	105.19(12)
N2–M–Cl2	90.82(6)	95.61(14)	98.10(6)	99.77(5)	97.72(11)
N3–M–Cl1	109.39(6)	114.27(13)	111.43(7)	115.02(5)	114.38(11)
N3–M–Cl2	102.81(6)	103.00(13)	99.48(6)	101.60(4)	101.47(12)
Cl1–M–Cl2	101.35(3)	97.19(6)	98.24(3)	96.92(2)	96.79(5)

of the sp^3 nitrogen (N4). The dihedral angle between the aryl plane linked to the imino group and the basal coordination plane N1–N2–N3 is 76.58° , indicating a twist away from the quinolinyl plane, *ie* approaching perpendicular.

Similar structural features were observed for the iron complex **Fe4**, however, the iron atom has a larger deviation (0.829 Å) from the basal coordination plane (Θ N1–N2–N3). Its molecular structure is available in the Supporting Information.

A similar pseudo square-pyramid geometry was also exhibited by the cobalt complexes **Co2**, **Co3** and **Co4**; the molecular structure of **Co2** is shown in Fig. 2 whilst the molecular structures of **Co3** and **Co4** are available in the Supporting Information. The three coordinated nitrogen atoms and one chloride which comprise the basal square are almost co-planar with deviations in the range 0.37–0.44 Å, and the cobalt atoms deviate from the basal plane at a distance of 0.447 Å (**Co2**), 0.385 Å (**Co3**) and 0.405 Å (**Co4**). The dihedral angles between the planes of the phenyl and the quinolyl rings are different (**Co2**: 87.75° ; **Co3**: 70.50° ; **Co4**: 54.55°), while the dihedral angles between the benzoimidazolyl and the quinolyl rings are 39.13° (**C2b**), 17.11° (**C3b**) and 20.00° (**C4b**), respectively.

**Fig. 1.** Molecular structure of complex **Fe1** with thermal ellipsoids at the 30% probability. Hydrogen atoms have been omitted for clarity.**Fig. 2.** Molecular structure of complex **Co2** with thermal ellipsoids at the 30% probability. Hydrogen atoms have been omitted for clarity.

3.3. Ethylene polymerization

Various alkylaluminum reagents were employed as co-catalysts with both the iron and cobalt pro-catalysts. Catalytic systems with methylaluminoxane (MAO) were found to exhibit the best catalytic activity in ethylene polymerization. As a consequence, activation employing MAO as co-catalyst was investigated in detail.

3.3.1. Ethylene polymerization by iron complexes

The pro-catalyst **Fe3** was typically investigated by varying various reaction parameters such as the reaction temperature, molar ratio of Al/Fe and the ethylene pressure. There was no activity observed at ambient temperature, and the catalytic system produced only trace polyethylene at 40°C . When the reaction temperature was elevated to 60°C or higher (runs 1–3, Table 3), ethylene polymerization occurred with good activity. The activities steadily increased with increased reaction temperature (runs 1–3, Table 3), whilst the molecular weights of the resultant polyethylenes gradually decreased and with narrower molecular weight distribution (Fig. 3). It was believed that the formation of

Table 3
Ethylene polymerization using iron Complexes.^a

Run	Pro-cat.	Al/Fe	T/ $^\circ\text{C}$	P/MPa	Activity ^b	PE yield/g	T_m ^c / $^\circ\text{C}$	M_w ^d ($\times 10^{-4}$)	M_w/M_n ^d
1	Fe3	3000	60	3	1.53	0.383	135.6	159.0	19.0
2	Fe3	3000	80	3	3.21	0.803	135.1	91.3	11.5
3	Fe3	3000	100	3	6.53	1.63	134.6	26.7	4.1
4	Fe3	1000	100	3	2.32	0.581	134.9	nd	nd
5	Fe3	2000	100	3	3.86	0.965	134.5	42.0	7.3
6	Fe3	2500	100	3	5.66	1.42	134.5	29.4	5.9
7	Fe3	3500	100	3	6.19	1.55	133.0	16.5	4.0
8	Fe3	3000	100	2	3.63	0.908	134.6	33.2	5.0
9	Fe3	3000	100	1	1.23	0.253	134.2	36.0	6.6
10	Fe1	3000	100	3	2.83	0.708	133.0	20.1	5.4
11	Fe2	3000	100	3	4.64	1.16	134.4	24.5	4.8
12	Fe4	3000	100	3	3.31	0.828	133.5	23.5	5.8
13	Fe5	3000	100	3	0.941	0.235	132.6	17.7	5.4
14	Fe6	3000	100	3	1.46	0.366	133.3	28.4	6.8

^a Conditions: 5 μmol Fe; polymerization time: 30 min; 100 mL toluene.^b $10^5 \text{ g mol}^{-1}(\text{Fe})\cdot\text{h}^{-1}$.^c Determined by DSC.^d Determined by GPC.

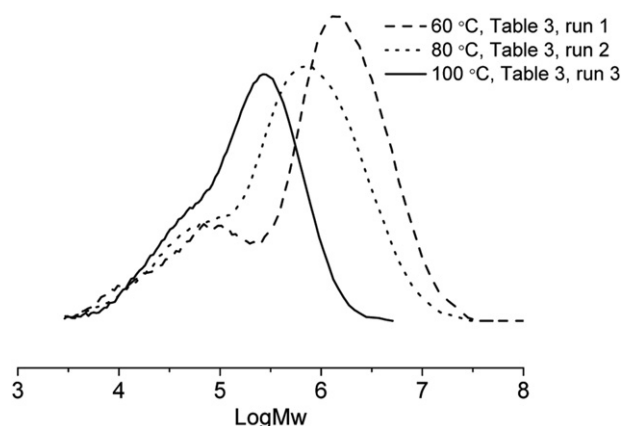


Fig. 3. The GPC curves of PEs produced by iron complexes at different reaction temperature.

the thermally stable active species required relatively high temperatures. Within bis(imino)pyridylmetal pro-catalysts, there are few examples of systems providing good activities at high temperature [32,41,52–54]; the current pro-catalysts provide an alternative model of tridentate iron pro-catalysts in ethylene polymerization.

The Al/Fe molar ratio was varied from 1000 to 3500 (runs 4–7, Table 3), the highest activity was observed with an Al/Fe of 3000. Though similar activities were observed over the Al/Fe range of 2500–3500, the molecular weights and distributions both decreased on employing a higher Al/Fe molar ratio (Fig. 4), indicative of chain transfer and termination from the iron-species to aluminum. According to the narrower molecular distribution of polyethylene obtained with higher Al/Fe molar ratios, common active species were present displaying similar catalytic processes.

Upon increasing the ethylene pressure (runs 3, 8 and 9, Table 3), the activities were increased, whilst lower molecular weights and narrower distributions of the resultant polyethylenes were observed with higher ethylene pressure (Fig. 5), indicating probable migration of the active species from the polymeric chain to the monomer.

In the following, the iron pro-catalysts with differing substituents were investigated for their catalytic performance (runs 3, 10–14, Table 3). The activities gradually increased on tuning the sterics of the group on the *ortho* position of imino phenyl ring, e.g. on going from a methyl group to an isopropyl group. The bulkier substituent could retard the effect of unwanted impurities and impart protection at the active species [1,2,9–14]. The introduction

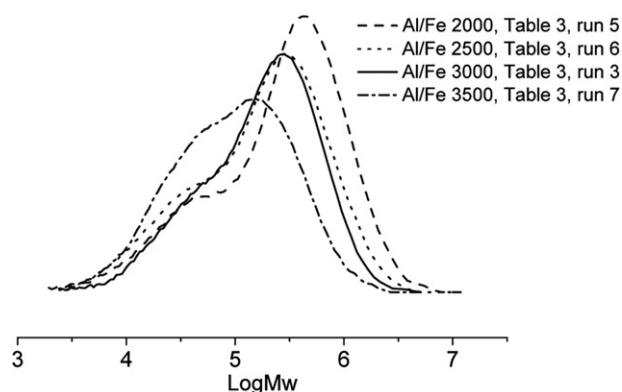


Fig. 4. The GPC curves of PEs obtained at different molar ratios of Al/Fe.

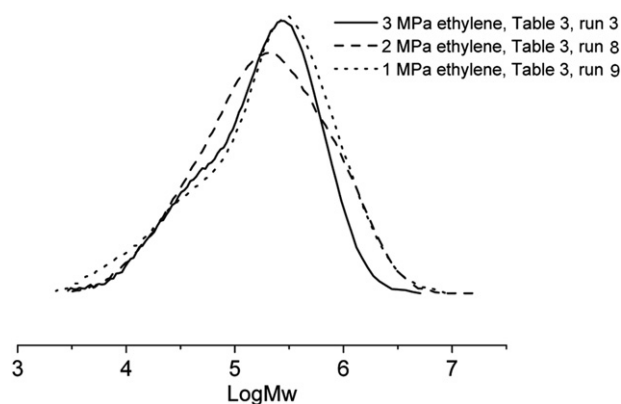


Fig. 5. The GPC curves of PEs produced by iron complexes at different ethylene pressure.

of a methyl group at the *para* position of the imino phenyl ring group increased the catalytic activities probably due to enhanced solubility properties. On changing the substituents at the *ortho* position of the imino phenyl ring from an alkyl group to a halogen group, the activities greatly decreased. In general, the molecular weight distributions of resultant polyethylenes were relatively broad, indicating multimodal features of the polymers formed, and also more than one active species [55–70]. Checking the influences of the ligand environment on the properties of polyethylenes (runs 3, 10–14, Table 3), the molecular weights of the resultant polyethylenes gradually increased in the order of $L1 < L2 < L3$ due to the bulky effect of substituents on arylimino ring, and the M_w obtained by **C6** ($R^1 = Cl$) was higher than that obtained by **C5** ($R^1 = F$). At the same time, the introduction of a methyl group at the *para* position of the imino phenyl ring group also slightly increased the molecular weights. Similar trends also could be found for the cobalt complexes.

3.3.2. Ethylene polymerization by cobalt pro-catalysts

When using the **Co3**/MAO system (runs 1–9, Table 4), similar to the catalytic system **Fe3**/MAO, the higher the reaction temperature used (runs 1–3, Table 4), the higher the catalytic activities observed, but the lower the molecular weight and the narrower molecular weight distribution of the polyethylene obtained. The higher the Al/Fe molar ratio employed, the lower the molecular weight and the narrower the molecular weight distribution of polyethylene formed. The best activity was observed at the Al/Fe of 3000. The higher the ethylene pressure used (runs 3, 8 and 9, Table 4), the higher the catalytic activity observed, but the lower the molecular weight of the polyethylene obtained.

All the other cobalt pro-catalysts were investigated using these optimum polymerization conditions (runs 3, 10–14, Table 4). The catalytic activities were observed to be in the order $Co3 > Co2 > Co4 > Co1$ and $Co6 > Co5$, consistent with the performance of their iron analogs, and again, pro-catalysts bearing halo-substituents at the *ortho* position of the imino phenyl ring exhibited lower activities than did their analogs bearing alkyl-substituents. Compared with the iron complexes, the cobalt complexes exhibited slightly lower catalytic activities; the M_w obtained by the cobalt complexes were equal to those of the iron complexes. In general, the Fe catalysts are more active than the corresponding Co analogues in bis(imino)pyridine system [1–6]. The nature of the metal center has a large influence on catalyst performance. However, catalyst performance is also strongly dependent on the nature of the donor atoms, the electronic and steric effects of the substituents, and the nature of the chelate ligand.

Table 4
Ethylene polymerization using the cobalt Pro-catalysts.^a

Run	Complex	Al/Co	T/°C	P/MPa	Activity ^b	PE/g	T _m ^c /°C	M _w ^d (× 10 ⁻⁴)	M _w /M _n ^d
1	Co3	3000	60	3	1.08	0.269	135.6	nd	nd
2	Co3	3000	80	3	2.11	0.529	135.3	122.7	14.7
3	Co3	3000	100	3	4.05	1.01	134.1	29.0	6.2
4	Co3	1000	100	3	0.963	0.241	135.1	nd	nd
5	Co3	2000	100	3	2.83	0.708	134.6	34.2	5.2
6	Co3	2500	100	3	3.39	0.848	134.3	29.2	6.2
7	Co3	3500	100	3	3.88	0.969	132.5	24.4	6.4
8	Co3	3000	100	2	2.67	0.668	134.5	29.5	6.3
9	Co3	3000	100	1	1.01	0.253	134.8	39.2	6.4
10	Co1	3000	100	3	2.33	0.583	133.3	21.3	4.8
11	Co2	3000	100	3	3.67	0.918	133.6	25.4	4.7
12	Co4	3000	100	3	3.03	0.758	133.6	22.1	4.7
13	Co5	3000	100	3	0.663	0.189	133.3	18.2	4.0
14	Co6	3000	100	3	0.936	0.234	134.1	25.9	5.5

^a Conditions: 5 μmol Co; polymerization time: 30 min; 100 mL toluene.^b 10⁵ g mol⁻¹(Co)·h⁻¹.^c Determined by DSC.^d Determined by GPC.

4. Conclusion

The series of iron(II) and cobalt(II) complexes bearing 2-(1-(arylimino)methyl)-8-(1*H*-benzimidazol-2-yl)quinoline ligands were synthesized and fully characterized. X-ray diffraction studies confirmed the structural geometry at the metal as a distorted square-based pyramidal. Upon activation with MAO, the iron and the cobalt pro-catalysts all exhibited good activities in ethylene polymerization at 100 °C, indicating the thermal stability of the active species. Although the bulk of the ligands could enhance the catalytic activities of the metal pro-catalysts, lower molecular weights and narrower distributions of resultant polyethylenes were observed on increasing the ethylene pressure, indicating a probable exchange of chain with monomer on the active species.

Acknowledgment

Acknowledgements: This work was supported by MOST 863 program No. 2009AA034601. CR wishes to thank the EPSRC for an overseas travel grant (EP/H031855/1).

Supporting information available

Molecular structures of complexes **Fe4**, **Co3** and **Co4**, and other GPC diagrams of obtained polyethylenes.

Appendix. Supplementary data

Supplementary data related to this article can be found online at doi:10.1016/j.polymer.2011.10.037.

References

- [1] Small BL, Brookhart M, Bennett AMA. *J Am Chem Soc* 1998;120(16):4049–50.
- [2] Britovsek GJP, Gibson VC, Kimberley BS, Maddox PJ, McTavish SJ, Solan GA, et al. *Chem Commun* 1998;7:849–50.
- [3] Gibson VC, Spitzmesser SK. *Chem Rev* 2003;103(1):283–315.
- [4] Gibson VC, Redshaw C, Solan GA. *Chem Rev* 2007;107(5):1745–76.
- [5] Bianchini C, Giambastiani G, Rios IG, Mantovani G, Meli A, Segarra AM. *Coord Chem Rev* 2006;250(11–12):1391–418.
- [6] Bianchini C, Giambastiani G, Luconi L, Meli A. *Coord Chem Rev* 2010;254(5–6):431–55.
- [7] Sun WH, Zhang S, Zuo W. *C R Chim* 2008;11(3):307–16.
- [8] Jie S, Sun WH, Xiao T. *Chin J Polym Sci* 2010;28(3):299–304.
- [9] Britovsek GJP, Bruce M, Gibson VC, Kimberley BS, Maddox PJ, Mastroianni S, et al. *J Am Chem Soc* 1999;121(38):8728–40.
- [10] Britovsek GJP, Mastroianni S, Solan GA, Baugh SPD, Redshaw C, Gibson VC, et al. *Chem Eur J* 2000;6(12):2221–31.
- [11] Chen Y, Qian C, Sun J. *Organometallics* 2003;22(6):1231–6.

- [12] Paulino IS, Schuchardt U. *J Mol Catal A Chem* 2004;211(1):55–8.
- [13] Zhang Z, Chen S, Zhang X, Li H, Ke Y, Lu Y, et al. *J Mol Catal A Chem* 2005;230(1):1–8.
- [14] Liu JY, Zheng Y, Li YG, Pan L, Li YS, Hu NH. *J Organomet Chem* 2005;690(5):1233–9.
- [15] Sun WH, Jie S, Zhang S, Zhang W, Song Y, Ma H. *Organometallics* 2006;25(3):666–77.
- [16] Jie S, Zhang S, Sun WH, Kuang X, Liu T, Guo J. *J Mol Catal A Chem* 2007;269(1–2):85–96.
- [17] Jie S, Zhang S, Wedeking K, Zhang W, Ma H, Lu X, et al. *C R Chim* 2006;9(11–12):1500–9.
- [18] Jie S, Zhang S, Sun WH. *Eur J Inorg Chem* 2007;35:5584–98.
- [19] Zhang M, Zhang W, Xiao T, Xiang JF, Hao X, Sun WH. *J Mol Catal A Chem* 2010;320(1–2):92–6.
- [20] Zhang M, Hao P, Zuo W, Jie S, Sun WH. *J Organomet Chem* 2008;693(3):483–91.
- [21] Sun WH, Hao P, Zhang S, Shi Q, Zuo W, Tang X, et al. *Organometallics* 2007;26(10):2720–34.
- [22] Chen Y, Hao P, Zuo W, Gao K, Sun WH. *J Organomet Chem* 2008;693(10):1829–40.
- [23] Xiao L, Gao R, Zhang M, Li Y, Cao X, Sun WH. *Organometallics* 2009;28(7):2225–33.
- [24] Hao P, Chen Y, Xiao T, Sun WH. *J Organomet Chem* 2010;695(1):90–5.
- [25] Gao R, Wang K, Li Y, Wang F, Sun WH, Redshaw C, et al. *J Mol Catal A Chem* 2009;309(1):166–71.
- [26] Gao R, Li Y, Wang F, Sun WH, Bochmann M. *Eur J Inorg Chem* 2009;27(27):4149–56.
- [27] Sun WH, Hao P, Li G, Zhang S, Wang W, Yi J, et al. *J Organomet Chem* 2007;692(21):4506–18.
- [28] Zhang S, Vystorop I, Tang Z, Sun WH. *Organometallics* 2007;26(9):2456–60.
- [29] Zhang S, Sun WH, Kuang X, Vystorop I, Yi J. *J Organomet Chem* 2007;692(23):5307–16.
- [30] Wang K, Wedeking K, Zuo W, Zhang D, Sun WH. *J Organomet Chem* 2008;693(6):1073–80.
- [31] Zhang S, Sun WH, Xiao T, Hao X. *Organometallics* 2010;29(5):1168–73.
- [32] Xiao T, Zhang S, Kehr G, Hao X, Erker G, Sun WH. *Organometallics* 2011;30(13):3658–65.
- [33] Xiao T, Hao P, Kehr G, Hao X, Erker G, Sun WH. *Organometallics* 2011;30(18):4847–53.
- [34] Liu JY, Li YS, Liu JY, Li ZS. *Macromolecules* 2005;38(7):2559–63.
- [35] Liu FS, Hu HB, Xu Y, Guo LH, Zai SB, Song KM, et al. *Macromolecules* 2009;42(20):7789–96.
- [36] Guo LH, Gao HY, Zhang L, Zhu FM, Wu Q. *Organometallics* 2010;29(9):2118–25.
- [37] Popeney CS, Rheingold AL, Guan Z. *Organometallics* 2009;28(15):4452–63.
- [38] Schmid M, Eberhardt R, Klinga M, Leskelä M, Rieger B. *Organometallics* 2001;20(11):2321–30.
- [39] Meinhard D, Wegner M, Kipiani G, Hearley A, Reuter P, Fischer S, et al. *J Am Chem Soc* 2007;129(29):9182–91.
- [40] Ionkin AS, Marshall W. *Organometallics* 2004;23(13):3276–83.
- [41] Yu J, Liu H, Zhang W, Hao X, Sun WH. *Chem Commun* 2011;47(11):3257–9.
- [42] Yu J, Huang W, Wang L, Redshaw C, Sun WH. *Dalton Trans* 2011;40(39):10209–14.
- [43] Helldörfer M, Backhaus J, Alt HG. *Inorg Chim Acta* 2003;351:34–42.
- [44] Helldörfer M, Backhaus J, Milius W, Alt HG. *J Mol Catal A Chem* 2003;193(1–2):59–70.
- [45] Schleis T, Spaniol TP, Okuda J, Heinemann J, Mülhaupt R. *J Organomet Chem* 1998;569(1–2):159–67.

- [46] Schleis T, Heinemann J, Spaniol TP, Mühlaupt R, Okuda J. *Inorg Chem Commun* 1998;1(11):431–4.
- [47] Alobaidi F, Ye Z, Zhu S. *Polymer* 2004;45(20):6823–9.
- [48] Li T, Zhang CH, Zhu FM, Wu Q. *J Appl Polym Sci* 2008;108(1):206–10.
- [49] Li L, Jeon M, Kim SY. *J Mol Catal A Chem* 2009;303(1–2):110–6.
- [50] Provided by Astatech, Inc. (www.astatechinc.com).
- [51] Sheldrick GM. SHELXTL-97, program for the refinement of crystal structures. Germany: University of Gottingen; 1997.
- [52] Ionkin AS, Marshall WJ, Adelman DJ, Fones BB, Fish BM, Schiffhauer MF, et al. *J Polym Sci A Polym Chem* 2008;46(2):585–611.
- [53] Ionkin AS, Marshall WJ, Adelman DJ, Fones BB, Fish BM, Schiffhauer MF. *Organometallics* 2008;27(8):1902–11.
- [54] Ionkin AS, Marshall WJ, Adelman DJ, Fones BB, Fish BM, Schiffhauer MF. *Organometallics* 2008;27(6):1147–56.
- [55] Gibson VC, Humphries MJ, Tellmann KP, Wass DF, White AJP, Williams DJ. *Chem Commun* 2001;21:2252–3.
- [56] Britovsek GJP, Clentsmith GKB, Gibson VC, Goodgame DML, McTavish SJ, Pankhurst QA. *Catal Commun* 2002;3(5):207–11.
- [57] Bryliakov KP, Semikolenova NV, Zakharov VA, Talsi EP. *Organometallics* 2004;23(22):5375–8.
- [58] Bryliakov KP, Semikolenova NV, Zudin VN, Zakharov VA, Talsi EP. *Catal Commun* 2004;5(1):45–8.
- [59] Cámpora J, Naz AM, Palma P, Álvarez E, Reyes ML. *Organometallics* 2005;24(20):4878–81.
- [60] Bouwkamp MW, Lobkovsky E, Chirik PJ. *J Am Chem Soc* 2005;127(27):9660–1.
- [61] Bart SC, Chlopek K, Bill E, Bouwkamp MW, Lobkovsky E, Neese F, et al. *J Am Chem Soc* 2006;128(42):13901–12.
- [62] Wallenhorst C, Kehr G, Luftmann H, Fröhlich R, Erker G. *Organometallics* 2008;27(24):6547–56.
- [63] Trovitch RJ, Lobkovsky E, Chirik PJ. *J Am Chem Soc* 2008;130(35):11631–40.
- [64] Cruz VL, Ramos J, Martínez-Salazar J, Gutiérrez-Oliva S, Toro-Labbé A. *Organometallics* 2009;28(20):5889–95.
- [65] Raucoules R, Bruin T, Raybaud P, Adamo C. *Organometallics* 2009;28(18):5358–67.
- [66] Bryliakov KP, Talsi EP, Semikolenova NV, Zakharov VA. *Organometallics* 2009;28(11):3225–32.
- [67] Bowman AC, Milsmann C, Atienza CCH, Lobkovsky E, Wieghardt K, Chirik PJ. *J Am Chem Soc* 2010;132(5):1676–84.
- [68] Bowman AC, Milsmann C, Bill E, Lobkovsky E, Weyhermüller T, Wieghardt K, et al. *Inorg Chem* 2010;49(13):6110–23.
- [69] Tondreau AM, Milsmann C, Patrick AD, Hoyt HM, Lobkovsky E, Wieghardt K, et al. *J Am Chem Soc* 2010;132(42):15046–59.
- [70] Atienza CCH, Bowman AC, Lobkovsky E, Chirik PJ. *J Am Chem Soc* 2010;132(46):16343–5.